Transport properties of single-crystalline Cu_xTiSe_2 ($0.015 \leqslant x \leqslant 0.110$)

G. Wu, H. X. Yang, L. Zhao, X. G. Luo, T. Wu, G. Y. Wang, and X. H. Chen*

Hefei National Laboratory for Physical Science at Microscale and Department of Physics, University of Science and Technology of China, Hefei, Anhui 230026, People's Republic of China

(Received 12 March 2007; revised manuscript received 19 May 2007; published 23 July 2007)

Transport properties are systematically studied for single crystals of Cu_xTiSe_2 ($0.015 \leqslant x \leqslant 0.110$). Both the in-plane and out-of-plane resistivity show a wide peak due to charge density waves (CDWs) for single crystals with $x \leqslant 0.025$. After the CDW state is completely suppressed around $x=0.055$, the superconductivity is apparently enhanced by Cu doping. No superconducting transition is observed above 1.8 K for $Cu_{0.11}TiSe_2$. The anisotropy in the resistivity increases with increasing Cu content, and is nearly T independent. The CDW state has a strong effect on the Hall coefficient and thermopower. Large thermopower, comparable to that of the triangular lattice Na_xCoO_2, is observed in Cu_xTiSe_2. Intercalation of Cu induces a negative magnetoresistance due to the interaction between conducting carriers and localized magnetic moments.

DOI: 10.1103/PhysRevB.76.024513 PACS number(s): 74.25.Fy, 74.70.Dd, 71.45.Lr

INTRODUCTION

Layered transition metal dichalcogenides (TMD's) MX_2 (M=transition metal, X=S, Se, or Te) have been extensively studied due to their two-dimensional structure and physical properties, such as superconductivity and a charge density wave (CDW) transition.[1–3] The structure of these compounds usually manifests two phases, 1T and 2H phase; structures are formed by X-M-X sandwiches. The top and bottom sheets are chalcogen atoms, and the middle sheets are metal atoms. In the 1T phase, all the sandwiches stack on each other octahedrally, while in the 2H phase, the sandwiches stack in a trigonal prismatic way.[1] The CDW state is one of the most interesting phenomena observed in TMD's and widely studied. Superconductivity also appears in some materials, such as 2H-NbS_2 which is a multigap s-wave superconductor. The coexistence of superconductivity and CDW state has been widely observed in 2H transition metal dichalcogenides $TaSe_2$, TaS_2, and $NbSe_2$. 2H-$TaSe_2$ experiences incommensurate and a commensurate CDW transitions at 122 and 90 K, respectively; 2H-TaS_2 and 2H-$NbSe_2$ undergo only one incommensurate CDW transition at 75 and 35 K, respectively; while 2H-NbS_2 shows no CDW transition.[1,3,4] In contrast to the CDW transition, the superconducting transition temperature decreases from 2H-$TaSe_2$, through 2H-TaS_2 and 2H-$NbSe_2$, to 2H-NbS_2, indicating that the CDW state and superconductivity compete with each other.

The interaction between the layers of TMD's is of weak van der Waals type, so that this kind of compound can be easily intercalated by various guest species (e.g., alkali-metal atoms, 3d transition metal atoms, or molecules).[5–7] The lattice parameters are usually changed by intercalation; a superstructure can be observed at some guest concentrations.[3,8] Such a superstructure is related to the CDW state. Recently, it has been found that intercalation of Na into 2H-TaS_2 increases the superconducting transition temperature to 5 K, and suppresses the CDW transition.[9–11] The effect of pressure on superconductivity and the CDW state shows results in 2H-$NbSe_2$.[12] These results further indicate that the superconductivity and CDW state compete with each other.[3,13]

The intercalation of various guest atoms into van der Waals gaps of MX_2 is another way to study TMD's and to find new phenomena. Recently, Cu has been successfully intercalated into 1T-$TiSe_2$.[14] Intercalation of Cu continuously suppresses the CDW transition; superconductivity emerges in the sample Cu_xTiSe_2 with $x \sim 0.04$, and reaches a maximum transition temperature (T_c) of 4.15 K at $x=0.08$; then T_c decreases with further doping Cu.[14] The phase diagram of Cu_xTiSe_2 is quite similar to that of high-T_c cuprates. Therefore, it is of great interest to see if unconventional superconductivity exists in Cu_xTiSe_2 system. Cu_xTiSe_2 is the first superconducting 1T structured MX_2 compound. $TiSe_2$ intercalated with other 3d transition metals (e.g., V, Cr, Mn, Fe, Co, Ni) has been reported, but no superconductivity is observed.[8,15] Study of the anisotropic properties of $Cu_{0.07}TiSe_2$ shows that it is a normal type-II superconductor.[16] The results of thermal conductivity for $Cu_{0.06}TiSe_2$ indicate that it is a single-gap s-wave superconductor.[17] Angle-resolved photoemission spectroscopy results show that intercalation of Cu could enhance the density of states, leading to superconductivity, but excessive Cu makes the superconductivity disappear due to strong inelastic scattering.[18] In order to understand the CDW state and superconductivity in the Cu_xTiSe_2 system, we made a detailed study of the transport properties on high-quality single crystals of Cu_xTiSe_2. It is found that the CDW state has an observable effect on resistivity, Hall coefficient, and thermopower. Anisotropy in resistivity increases with increasing Cu content, and is nearly T independent, indicating the same scattering mechanism in the ab plane and along the c axis in Cu_xTiSe_2.

EXPERIMENTAL DETAILS

High-quality Cu_xTiSe_2 single crystals were grown by the chemical iodine-vapor transport method. Powders of Cu (99.7%), Ti (99.5%), and Se (99.5%) were mixed and thoroughly ground, then pressed into a pellet. The pellet was sealed under vacuum in a quartz tube with diameter of 13 mm and length of 150 mm with iodine (10 mg/cm^{-3}). One end of the tube was slowly heated to 940 °C with heat-

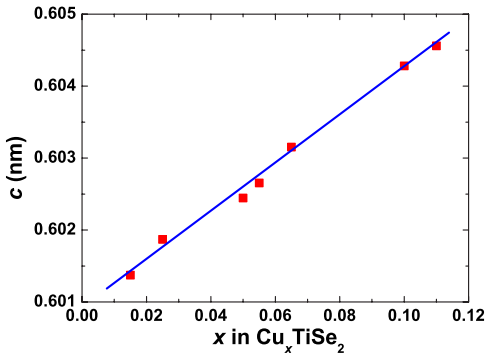

FIG. 1. (Color online) c-axis lattice parameter as a function of x in Cu_xTiSe_2 for single crystals, consistent with that reported in polycrystalline samples (Ref. 14). The straight line guides the eyes.

ing rate of ~150 °C/h; the other end at 740 °C. After one week, the furnace was cooled to room temperature over a few hours. Finally, many golden platelike Cu_xTiSe_2 crystals were obtained. The typical dimension is about $5\times5\times0.03$ mm^3. Because the element Cu can react with Se very easily, excess Cu was used as starting material. For example, in order to grow $Cu_{0.055}TiSe_2$ crystals, the molar stoichiometry of the Cu, Ti, and Se powder is 0.4:1:2. The actual composition of the single crystals was determined by x-ray fluorescence spectroscopy (XRF-1800, Shimadzu Inc.)

All crystals were characterized with a Rigaku D/max-A x-ray diffractometer with graphite-monochromatized Cu $K\alpha1$ radiation ($\lambda=1.5406$ Å) in the 2θ range of 10°–70° with steps of 0.02° at room temperature. Resistivity measurements were performed on an ac resistance bridge (Linear Research, Inc., Model LR700) by the standard four-probe method. The magnetic field was supplied by a superconducting magnet system (Oxford Instruments). The Hall contact configuration is the standard ac six-probe geometry. To eliminate the offset voltage due to the asymmetric Hall terminals, the magnetic field was scanned from −5 to 5 T. Thermopower measurements were carried out with a home-built apparatus and performed using small and reversible temperature differences of 0.5 K. Two ends of the single crystals were attached to two separated copper heat sinks to generate the temperature gradient along the crystal ab plane. Two Rh-Fe thermometers were glued to the heat sink (next to the single crystals). Copper leads were adhered to the single crystals and all the data were corrected for the contribution of the Cu leads.

RESULTS AND DISCUSSION

Figure 1 shows the c-axis lattice parameter as a function of Cu content (x). The c-axis lattice parameter was obtained by x-ray diffraction on single crystals of Cu_xTiSe_2 with different x. It shows a good relationship between the c-axis lattice parameter and Cu content. The c-axis lattice parameter increases linearly with increasing Cu content. This is consistent with the results reported in polycrystalline samples.[14]

Figure 2 shows the temperature dependence of the in-plane resistivity ρ_{ab} from 300 to 2 K for Cu_xTiSe_2 crystals with different Cu content (x=0.015, 0.025, 0.055, 0.065, 0.08, 0.10, and 0.11). As show in Fig. 2, ρ_{ab} shows a wide peak due to the CDW for samples with $x\leqslant0.025$; the CDW peak becomes broader and moves to lower temperature with increasing x. This indicates that the intercalation of Cu suppresses the CDW, the observations consistent with that of Morosan *et al.*[14] For the sample with x=0.055, the CDW peak disappears and the resistivity becomes nearly T^2 dependent. This suggests that the CDW state is completely suppressed around x=0.055. The fact that intercalation of Cu leads to suppression of the CDW state could be related to the structural change induced by Cu doping. In $TiSe_2$, the $TiSe_2$ goes through a $2\times2\times2$ structural transition below 200 K, leading to a CDW state.[19,20] The CDW state has a close relationship with the structure of $TiSe_2$. When Cu is intercalated into the $TiSe_2$ layers, such a $2\times2\times2$ lattice is destroyed. The disorder of the Cu atoms destroys the superlattice of $TiSe_2$, leading to suppression of the CDW state.

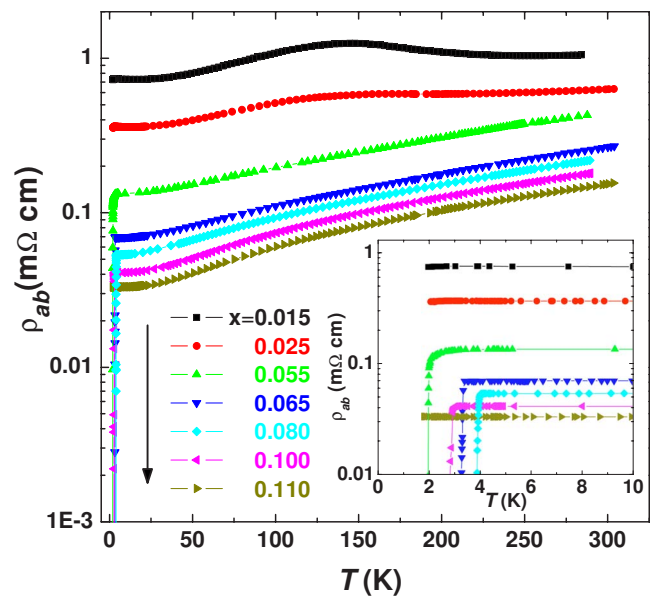

FIG. 2. (Color online) Temperature dependence of in-plane resistivity down to 2 K for Cu_xTiSe_2 crystals with different Cu content. The low-temperature $\rho(T)$ data are plotted in the inset.

The resistivity monotonically decreases with increasing Cu content. The residual resistivity ratio $\rho_{ab}(300\text{ K})/\rho_{ab}(5\text{ K})$ increases from ~2 to ~5 with increasing Cu content from 0.015 to 0.11. These results are consistent with those reported in polycrystalline samples.[14] In order to clearly show the superconducting transition, the low-temperature $\rho_{ab}(T)$ data were plotted in the inset of Fig. 2. The superconducting transition temperature (T_{onset}) is 2.24, 3.40, 4.13, and 3.02 K for the samples with x=0.055, 0.065, 0.08, and 0.10, respectively. It should be pointed out that the superconducting transition is not observed in the sample with x=0.11 while cooling the sample to 1.8 K. These results are nearly consistent with the phase diagram obtained from polycrystalline samples.[14]

The temperature dependence of the out-of-plane resistivity ρ_c is plotted in Fig. 3(a) for samples of Cu_xTiSe_2 crystals

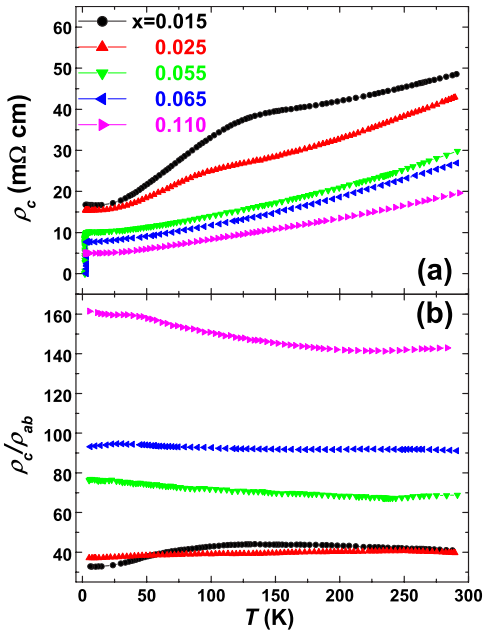

FIG. 3. (Color online) Temperature dependence of (a) out-of-plane resistivity for Cu_xTiSe_2 crystals with different Cu content; and (b) anisotropy in resistivity for Cu_xTiSe_2 crystals with different Cu content.

with different Cu content (x=0.015, 0.025, 0.055, 0.065, and 0.110). As shown in Fig. 3(a), $\rho_c(T)$ shows similar behavior to $\rho_{ab}(T)$. $\rho_c(T)$ monotonically decreases with increasing Cu content. An obvious CDW peak can be observed in $\rho_c(T)$ for slightly Cu-doped samples with $x \leqslant 0.025$. The CDW state is suppressed by intercalation of more Cu. $\rho_c(T)$ shows T^2-dependent behavior for the samples without a CDW state. The temperature dependence of the resistivity anisotropy ρ_c/ρ_{ab} is shown in Fig. 3(b) for samples of Cu_xTiSe_2 crystals with different Cu content (x=0.015, 0.025, 0.055, 0.065, and 0.110). ρ_c/ρ_{ab} shows a weak temperature dependence in all the samples with different Cu content. This indicates that the charge transport mechanism is the same in the *ab* plane and along Cu_xTiSe_2. Compared to the case of TiS_2, the anisotropy for the samples Cu_xTiSe_2 is smaller. In the case of TiS_2 the resistivity anisotropy is 1500 and 750 at 5 and 300 K, respectively.[21] In Cu_xTiSe_2, Se has a larger radius and stronger covalence than S, so that the carriers can move more easily between the layers in Cu_xTiSe_2 than in TiS_2. With intercalation of Cu, the in-plane conductivity is strongly enhanced over the *c*-axis conductivity, so that the anisotropy increases with increasing x in Cu_xTiSe_2. A similar enhancement of anisotropy with increasing carrier content is observed in *n*-type cuprates.[22]

Figure 4 shows the temperature dependence of the in-plane thermopower (S) for the Cu_xTiSe_2 crystals with x =0.015, 0.065, and 0.110. The thermopower is negative in the whole temperature range. This indicates that the carrier is *n* type. At room temperature, the magnitude of S decreases with increasing x. The thermopower shows a nonmonotonic temperature dependence for the sample $Cu_{0.015}TiSe_2$; a maximum value of S appears at 150 K at which a CDW transition is observed in resistivity. This suggests that the nonmonotonic T dependence for S arises from the occurrence of CDW order. For the samples without a CDW state, the magnitude of S monotonically decreases with decreasing temperature. All these results indicate that the metallic nature of Cu_xTiSe_2 is enhanced by electron doping. It should be pointed out that the thermopower is anomalously large. Compared to the triangular lattice Na_xCoO_2 with large thermopower, Cu_xTiSe_2 shows a larger S^2/ρ_{ab} at room temperature than Na_xCoO_2. In $Cu_{0.065}TiSe_2$, $S(300\text{ K}) \simeq 60\ \mu\text{V/K}$ and $\rho_{ab}(300\text{ K}) \simeq 0.15\ \text{m}\Omega\text{ cm}$; while for $Na_{0.68}CoO_2$, $S(300\text{ K}) \simeq 90\ \mu\text{V/K}$ and $\rho_{ab}(300\text{ K}) \simeq 1\ \text{m}\Omega\text{ cm}$.[23] In this sense, Cu_xTiSe_2 has a larger power factor than Na_xCoO_2. In the Na_xCoO_2 system, the anomalously large thermopower is ascribed to the contribution of spin entropy.[24] Therefore, the anomalously large thermopower in the Cu_xTiSe_2 system deserves further investigation.

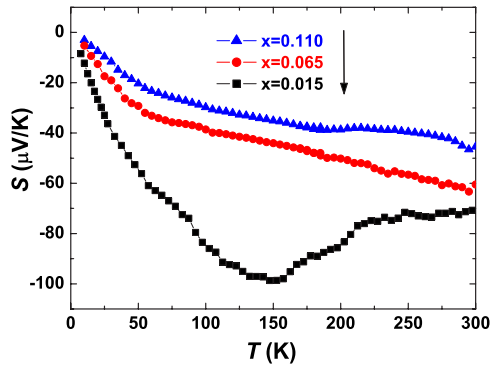

FIG. 4. (Color online) Temperature dependence of the in-plane thermopower for the samples Cu_xTiSe_2 with x=0.015, 0.065, 0.110.

Figure 5 shows the temperature dependence of the Hall coefficient (R_H) for Cu_xTiSe_2 with x=0.015, 0.025, 0.065, 0.110. In the whole temperature range, R_H is negative. Both the thermopower and the Hall coefficient indicate that the carrier is *n* type in the Cu_xTiSe_2 system. The Hall coefficient decreases with increasing Cu content. This indicates that the carrier concentration increases with Cu doping, consistent with the results of resistivity and thermopower. The samples with a CDW state show a strongly temperature-dependent R_H behavior. The Hall coefficient shows a strong T dependence below 200 K for the sample with x=0.015, and below 100 K for the sample with x=0.025. These results coincide with the

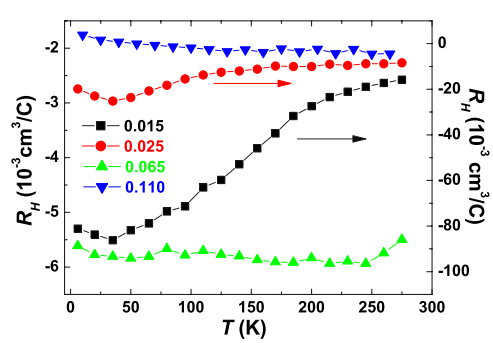

FIG. 5. (Color online) Temperature dependence of the Hall coefficient (R_H) for samples of Cu_xTiSe_2 with x=0.015, 0.025, 0.065, 0.110.

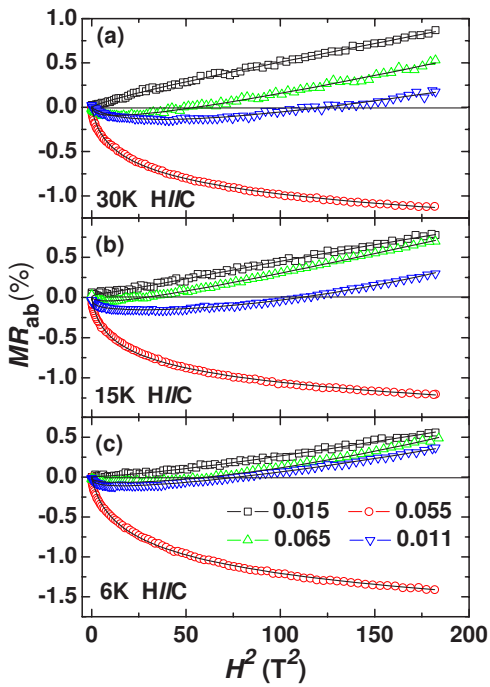

FIG. 6. (Color online) Isothermal magnetoresistance at 6, 15, and 30 K for the samples Cu_xTiSe_2 with $x=0.015$, 0.055, 0.065, 0.110.

occurrence of CDW order observed in resistivity. For the samples without a CDW state, the Hall coefficient shows T-independent behavior within the uncertainty. This indicates characteristics of a metal for the heavily Cu-doped sample. It further indicates that the T-dependent Hall coefficient arises from the CDW state. Formation of the CDW state leads to localization of some carriers, so that the number of conducting carriers decreases, and consequently enhances the Hall coefficient. This is why the R_H increases below 200 and 100 K for the samples with $x=0.015$ and 0.025 as shown in Fig. 5.

Figure 6 shows the H^2 dependence of isothermal in-plane magnetoresistance (MR) with magnetic field along the c axis for Cu_xTiSe_2 with $x=0.015$, 0.055, 0.065, and 0.110 at 6, 15, and 30 K. For the sample with $x=0.015$, the isothermal MR is positive in the whole magnetic field range, and shows a good H^2-dependent behavior at different temperatures. It implies that the isothermal MR just comes from the contribution of the Lorentz force to the carriers under a magnetic field. However, the isothermal MR shows a complicated magnetic field (H) dependence for the samples with $x=0.065$ and 0.110. The MR is negative and increases with increasing H at low magnetic field; then decreases and crosses zero at a certain H; the positive MR increases with increasing H at high magnetic field. This indicates that the MR comes from two contributions: one negative and one positive component. As shown in Fig. 6, the isothermal MR shows almost H^2 dependence at high H for the samples with $x=0.065$ and 0.110. It suggests that the MR is dominated by the Lorentz force. In order to understand the complicated MR, the formula $\Delta\rho/\rho=-A_1^2\ln(1+A_2^2H^2)+B_1^2H^n$ is used to fit the experimental data. The first term in the formula comes from a semiempirical expression proposed by Khosla and Fischer[25] and has been used to explain the negative MR. The basis for this formula is Toyazawa's localized-magnetic-moment model of magnetoresistance, where carriers in an impurity band are scattered by the localized spin of impurity atoms.[26] It is found that all data can be well fitted by the formula for all samples. This indicates that the negative MR comes from the interaction between conducting carriers and localized magnetic moments. It reveals a decrease of spin-dependent scattering of carriers in magnetic fields. When Cu is intercalated into the $TiSe_2$ layers, some of the nonmagnetic Ti(IV) ions change into magnetic Ti(III), so that interaction between conducting carries and localized magnetic moments takes place. This interaction between conducting carriers and localized magnetic moments results in a negative contribution to the MR. Therefore, the complicated H-dependent MR can be well understood. However, an anomalous MR is observed for the sample with $x=0.055$ compared to the observation of MR in other samples. The sample with $x=0.055$ shows negative MR in the whole H range, and the negative MR monotonically increases with increasing H. This indicates that the MR is dominated by the interaction between conducting carries and localized magnetic moments even at high magnetic field. This anomaly could be related to the critical point for disappearance of the CDW state.

CONCLUSION

In conclusion, we have grown high-quality Cu_xTiSe_2 single crystals with different Cu content from $x=0.015$ to 0.110. The transport properties, anisotropic resistivity, thermoelectric power, Hall coefficient, and magnetoresistivity have been systematically studied. A systematic evolution of the CDW state and the superconducting state with Cu content is observed. It is found that the CDW state can be suppressed by intercalation of Cu, while superconductivity is induced. The CDW state gives a strong effect on the transport properties, leading to T-dependent Hall coefficient. An anomalously large thermopower is observed, even comparable to that of the large-thermopower material Na_xCoO_2. It deserves further study. Intercalation of Cu induces a negative MR due to the interaction between conducting carriers and localized magnetic moments.

ACKNOWLEDGMENTS

This work is supported by a grant from the Natural Science Foundation of China and by the Ministry of Science and Technology of China (973 Project No. 2006CB601001) and by the National Basic Research Program of China (Grant No. 2006CB922005).

*Corresponding author. chenxh@ustc.edu.cn

[1] J. A. Wilson, F. J. Di Salvo, and S. Mahajan, Adv. Phys. **24**, 117 (1975).
[2] R. H. Friend and A. D. Yoffe, Adv. Phys. **36**, 1 (1987).
[3] J. A. Wilson and A. D. Yoffe, Adv. Phys. **18**, 193 (1969).
[4] D. E. Moncton, J. D. Axe, and F. J. DiSalvo, Phys. Rev. B **16**, 801 (1977).
[5] M. S. Whittingham, Prog. Solid State Chem. **12**, 41 (1978).
[6] M. S. Whittingham, J. Electrochem. Soc. **123**, 315 (1976).
[7] L. Trichet, J. Rouxel, and M. M. Pouchard, J. Solid State Chem. **14**, 283 (1975).
[8] Masasi Inoue and Hiroshi Negishi, J. Phys. Chem. **90**, 235 (1986).
[9] L. Fang, Y. Wang, P. Y. Zou, L. Tang, Z. Xu, H. Chen, C. Dong, L. Shan, and H. H. Wen, Phys. Rev. B **72**, 014534 (2005).
[10] F. Sernetz, A. Lerf, and R. Schöllhorn, Mater. Res. Bull. **9**, 1597 (1974).
[11] A. Lerf, F. Sernetz, W. Biberacher, and R. Schöllhorn, Mater. Res. Bull. **14**, 797 (1979).
[12] H. Suderow, V. G. Tissen, J. P. Brison, J. L. Martínez, and S. Vieira, Phys. Rev. Lett. **95**, 117006 (2005).
[13] A. H. Castro Neto, Phys. Rev. Lett. **86**, 4382 (2001).
[14] E. Morosan, H. W. Zandbergen, B. S. Dennis, J. W. G. Bos, Y. Onose, T. Klimczuk, A. P. Ramirez, N. P. Ong, and R. J. Cava, Nat. Phys. **2**, 544 (2006).
[15] A. N. Titov, A. V. Kuranov, V. G. Pleschev, Yu. M. Yarmoshenko, M. V. Yablonskikh, A. V. Postnikov, S. Plogmann, M. Neumann, A. V. Ezhov, and E. Z. Kurmaev, Phys. Rev. B **63**, 035106 (2001).
[16] E. Morosan, Lu Li, N. P. Ong, and R. J. Cava, Phys. Rev. B **75**, 104505 (2007).
[17] S. Y. Li, Louis Taillefer, G. Wu, and X. H. Chen, arXiv:cond-mat/0701669 (unpublished).
[18] J. F. Zhao, H. W. Ou, G. Wu, B. P. Xie, Y. Zhang, D. W. Shen, J. Wei, L. X. Yang, J. K. Dong, X. H. Chen, and D. L. Feng, arXiv:cond-mat/0612091 (unpublished).
[19] T. E. Kidd, T. Miller, M. Y. Chou, and T.-C. Chiang, Phys. Rev. Lett. **88**, 226402 (2002).
[20] F. J. Di Salvo, D. E. Moncton, and J. V. Waszczak, Phys. Rev. B **14**, 4321 (1976).
[21] H. Imai, Y. Shimakawa, and Y. Kubo, Phys. Rev. B **64**, 241104(R) (2001).
[22] C. H. Wang, G. Y. Wang, H. B. Song, Z. Feng, S. Y. Li, and X. H. Chen, Supercond. Sci. Technol. **18**, 763 (2005).
[23] I. Terasaki, Y. Sasago, and K. Uchinokura, Phys. Rev. B **56**, R12685 (1997).
[24] Y. Y. Wang, N. S. Rogado, R. J. Cava, and N. P. Ong, Nature (London) **423**, 425 (2003).
[25] R. P. Khosla and J. R. Fisher, Phys. Rev. B **2**, 4084 (1970).
[26] Y. Toyazawa, J. Phys. Soc. Jpn. **17**, 986 (1992).